Article:
Shi, Y, Babatunde, A orcid.org/0000-0003-4730-9673, Bockelmann-Evans, B et al. (2 more authors) (2020) On-going nitrification in chloraminated drinking water distribution system (DWDS) is conditioned by hydraulics and disinfection strategies. Journal of Environmental Sciences, 96. pp. 151-162. ISSN 1001-0742

https://doi.org/10.1016/j.jes.2020.04.028

On-going Nitrification in Chloraminated Drinking Water Distribution System (DWDS) is Conditioned by Hydraulics and Disinfection Strategies

Yi Shi[1,2*], Akintunde Babatunde[2,3], Bettina Bockelmann-Evans[2], Qijie Li[2] and Liang Zhang[1]

1. National Engineering Laboratory for Cereal Fermentation Technology, Jiangnan University, Wuxi, Jiangsu, China. Email: shiyi0621@jiangnan.edu.cn
2. Discipline of Civil Engineering, Cardiff University, The Parade, Cardiff, CF24 3AA, UK.
3. School of Civil Engineering, University of Leeds, Leeds, LS2, 9JT, UK

Received

Revised

Accepted

Abstract

Within the drinking water distribution system (DWDS) using chloramine as disinfectant, nitrification caused by nitrifying bacteria is increasingly becoming a concern as it poses a great challenge for maintaining water quality. To investigate efficient control strategies, operational conditions including hydraulic regimes and disinfectant scenarios were controlled within a flow cell experimental facility. Two test phases were conducted to investigate the effects on the extent of nitrification of three flow rates (Q = 2, 6, and 10 L/min) and four disinfection scenarios (total Cl_2=1mg/L, Cl_2/NH_3-N=3:1; total Cl_2=1mg/L, Cl_2/NH_3-N=5:1; total Cl_2=5mg/L, Cl_2/NH_3-N=3:1; and total Cl_2=5mg/L, Cl_2/NH_3-N=5:1). Physico-chemical parameters and nitrification indicators were monitored during the tests. The characteristics of biofilm extracellular polymetric substance (EPS) were evaluated after the experiment. The main results from the study indicate that nitrification is affected by hydraulic conditions and the process tends to be severe when the fluid flow transforms from laminar to turbulent ($2300<Re<4000$). Increasing disinfectant concentration and optimizing Cl_2/NH_3-N mass ratio were found to inhibit nitrification to some extend when the system was running at turbulent condition (Q = 10L/min, Re = 5535). EPS extracted from biofilm that was established at the flow rate of 6 L/min had greater carbohydrate/protein ratio. Furthermore, several nitrification indicators were evaluated for their prediction efficiency and the results suggest that the change of nitrite, together with

total organic carbon (TOC) and turbidity can indicate nitrification potential efficiently.

Keywords

Nitrification

Drinking water distribution system (DWDS)

Biofilm

Hydraulics

Disinfection

---

*Corresponding author. E-mail: shiyi0621@jiangnan.edu.cn

Introduction

In modern drinking water distribution systems (DWDS), chlorine and chloramine are the two main disinfectants applied for securing water quality (Gagnon et al., 2004). Compared with chlorine, chloramine is more persistent in water and hence resulting in better overall disinfection (Norton and LeChevallier, 1997). However, the disinfection efficiency of chloramine has been observed to be highly affected by microbial composition in both biofilm and bulk water (LeChevallier et al., 1990; Zhang and Edwards, 2009). In chloraminated DWDS, free ammonia released from chloramine decay will serve as an energy source for indigenous autotrophic ammonia oxidizing bacteria (AOB) and nitrite oxidizing bacteria (NOB) (Pintar and Slawson, 2003). Growth of these microorganisms mediates the process of nitrification, resulting in production of nitrite and further decrease of available chloramine (Hoefel et al., 2005). This process will not only show considerable influence on the inactivation efficiency of chloramine and subsequently affect drinking water quality, but also promote microorganism assemblage and hence to increase the possibility of regrowth events in the distribution system (Kirmeyer et al., 1995).

In order to provide advice on controlling nitrification in DWDS, researchers have focused on investigating the relationship between the abundance of nitrifying bacteria and system physic-chemical conditions (Kirmeyer et al., 1995; Odell et al., 1996; Wolfe et al., 1990; Zhang et al., 2008; Zhang et al., 2009b). Free ammonia concentration, dissolved oxygen, temperature, light, pH and alkalinity have been observed to be related to the growth of nitrifiers (Wolfe and Lieu, 2001; Zhang et al., 2009a). Several other factors

relating to nitrification were identified as well, which include nutrients, pipe materials and house hold treatment methods (i.e. filtration) (Fleming et al., 2005, 2008; Zhang et al., 2009a).

Compared with heterotrophic bacteria, nitrifiers are chemoautotrophic and show relative slow growth rate, especially under oligotrophic condition (Pintar and Slawson, 2003). However, once nitrification is underway and becomes severe, the process is observed to be difficult to control or inhibit within the DWDS (Cunliffe, 1991; Odell et al., 1996; Sathasivan et al., 2008; Seidel et al., 2005). Traditional nitrification controlling strategies are aimed at inhibiting the activity of nitrifying bacteria by optimizing disinfectant schedules (Skadsen and Cohen, 2006). Utilities normally prevent nitrification by increasing the chlorine to ammonia nitrogen ratio and hence to limit the available free ammonium within distribution systems (Odell et al., 1996). Measures such as periodically flushing and temporally using breakpoint chlorination are also applied to control nitrification (Lieu et al., 1993; Odell et al., 1996). Though nitrification could be eliminated for a period within DWDS via these operational management, the event is always recurring. The persistence of nitrification might be attributed to the support from biofilm, which enhances the stability and disinfection resistance of nitrifiers (Furumai and Rittmann, 1994; Volk and LeChevallier, 1999).

It has been suggested that the most possible existence form of nitrifying bacteria in DWDS is the aggregated bacterial cluster within biofilm (Tarre and Green, 2004; Wilczak et al., 1996). To control nitrification, factors related to biofilm formation should be considered as well. Studies have indicated that biofilm accumulated in DWDS is highly affected by operational conditions (i.e. hydraulics, disinfectants) (Douterelo et al., 2013; Mi et al., 2015). In addition, the extracellular polymetric substance (EPS), which is a kind of matrix embed within the biofilm, has been suggested to serve as a protector that prevents interferences from outer environment (Fish et al., 2016; Xue et al., 2012). This structure contributes to the resistance ability of biofilm, including the accumulated microorganisms, to the increasing shear stress or disinfectant dose (Fish et al., 2017; Xue et al., 2013). Further studies have suggested that biofilm EPS characteristics are impacted by the hydraulic condition to which the biofilm is exposed (Fish et al., 2016). However, for better understanding of the further hazards brought by nitrification in chloraminated DWDS,

research is needed on the relationships between operational effects (hydraulics and disinfection strategies) on biofilm structure (EPS) and nitrification process.

The aim of this study was to investigate the effects of hydraulic regimes and disinfection strategies (increasing disinfectant dose and chlorine to ammonia nitrogen ratio) on nitrification in chloraminated DWDS, as well as on biofilm EPS structure. Additionally, we aimed to evaluate the change of water quality in association with different experimental conditions and therefore to provide possible suggestions for utilities in securing water safety.

1 Materials and Methods

1.1 Experimental setup and operating conditions

To simulate the drinking water distribution system, a flow cell facility was applied in current study. The details of the design and characteristics for flow cell unit are described in Shi et al. (2019). Before applying different hydraulic regimes and disinfection schemes, nitrification was established by introducing dechlorinated tap water with a high concentration of ammonia (50 mg/L NH_3-N). The operation conditions and monitoring methods of this stage are described in Shi et al. (2019). After a stable nitrification process was developed, the facility was adjusted to investigate different experimental conditions. The schematic diagram is shown on **Fig. 1**. For the research reported here, two test phases were conducted, which included three hydraulic regimes and four disinfection scenarios. Each of the test phases ran for 33 days. The detailed operational conditions are listed in **Table 1**.

The feed water was prepared by firstly adding chlorine (from a stock solution of 500 mg/L total chlorine) to dechlorinated water to achieve a final concentration of 1.0/5.0 Cl_2 mg/L. After 24 hr, the water was re-adjusted to the required concentration of chlorine and ammonia (from pure ammonium chloride) was added to maintain a total chlorine to total ammonia nitrogen ratio of 3:1/5:1.

The pH, dissolve oxygen (DO) and conductivity within each flow cell unit were monitored every day during the experiment. Water samples were collected regularly from each unit and analysed for total and free chlorine (Cl_2), nitrite-nitrogen (NO_2^--N), nitrate-nitrogen (NO_3^--N), free ammonia nitrogen (NH_3-N), total organic carbon (TOC) and total nitrogen (TN). Heterotrophic plate count (HPC) measurement and chloramine decay tests

were conducted twice a week.

1.2 Analytical methods

1.2.1 Physico-chemical parameter measurement

The measurements of pH, DO and conductivity were made using a benchtop meter (SevenExcellence S600) and probes. A HACH portable instrument was used for turbidity analysis in this test (HACH DR 900) based on standard method 2130 (APHA, 1998). Total and free chlorine, nitrite nitrogen, nitrate nitrogen and free ammonia nitrogen were measured using a Benchtop Spectrophotometer (DR3900, *Hach*-Lange) and relevant standard reagent assays (produced by *Hach* Lange). TOC and TN were measured by a TOC analyser (TOC-V_{CPH} *Shimadzu*). For each parameter, three subsamples were collected, and the average was used as the final value.

1.2.2 Bio-parameters

HPC was determined by R2A agar plate following the standard method 9215 (APHA 1998). The microbiological decay factor (F_m) evaluates the contribution of microbiology to the overall monochloramine decay in the bulk water, as described by Sathasivan et al. (2005). The method is outlined herein.

The water sample was divided into two subsamples. One was unfiltered and the second was filtered through a 0.2 μm filter for removal of possible microbiological agents. After filtration, a microbial inhibitor ($AgNO_3$) was added to the second subsamples at 100μg-Ag/L, to ensure monochloramine decay was caused by chemical means only. The two subsamples were then incubated at a constant temperature of 20°C without light. The monochloramine residual was measured regularly when the total chlorine residual in the unfiltered sample reached 0.5 mg/L.

First-order reaction kinetics is used to describe all decay rates in this method. The integrated form is given by Eq. (1):

$$C_{NH_2Cl} = C_{NH_2Cl,0} exp\,(-k_s t) \quad (1)$$

Where $C_{NH_2Cl,0}$ is the initial monochloramine concentration in mg/L (i.e., at t=0), C_{NH_2Cl} is the monochloramine concentration in mg/L, k_S is the first-order decay coefficient of sample S at 20°C, and t is elapsed time in hours.

The decay coefficients for unfiltered and filtered (0.2 μm) with $AgNO_3$ sub-sample are k_{total} and k_C respectively. The difference between chemical decay (k_C) and total decay

(k_{total}) is attributable to microbiological agents including nitrifiers. The difference is defined as the microbial decay coefficient and is denoted as k_m (Eq. (2)).

$$K_m = k_t - k_c \quad (2)$$

F_m is the ratio of the microbial decay rate coefficient (k_m) and the chemical decay rate coefficient (k_C) as shown in equation Eq. (3).

$$F_m = \frac{k_m}{k_C} \quad (3)$$

1.3 Biofilm EPS extraction and characterisation

To characterise the biofilm EPS, coupons installed in each discrete flow cell (five for each) were collected after the experimental phases 1 and 2. In order to remove the attached biofilm thoroughly, the coupon was immersed into 10mL sterilized phosphate-buffered saline (PBS) and then sonicated in an ultrasonic water bath (Kerry 2593) for 10 mins at approximately 50 Hz. After all the five coupons were washed, the 10mL suspended culture was divided into two subsamples: 9 mL suspension was centrifuged to cell pellets for EPS extraction and quantification; the remaining 1 mL solution was for HPC counting and storage (combined with 20% glycerine).

The protocol used within the current study for EPS extraction is as described by Brown and Lester (1980). From the sub-sample collected in the last step, the cell pellets were firstly washed with 0.25 mL PBS and then re-suspended in 1.25 mL PBS. Combined with the 0.25 mL suspension from the washing step, the 1.5 mL suspension was transferred to a clean centrifuge tube and then 1.5 mL of 2% ethylenediaminetetraacetic acid (EDTA) in PBS was added. The solution was then sonicated for 30 s (Kerry 2593) and incubated for 3 hr at 4°C. After the incubation period, the solution was centrifuged at 20,000×g for 20 mins to pellet the cells. The supernatant was then filtered through 0.2 μm filters to remove possible microorganisms before EPS evaluation.

Total protein and carbohydrate were the two components from extracted EPS quantified within the current study. The total concentration of protein was determined using the standard Bradford assay (*Sigma* B6916) with bovine serum albumin (BSA) as standard. The total carbohydrate concentration within extracted EPS was measured using a standard phenol-sulphuric acid-based assay kit (*Sigma* MAK104) with glucose (2.0mg/l solution) as standard.

1.4 Statistical Analysis

Statistical analysis were performed using PASW Statistics 18.SPSS. As the water quality parameters were not normally distributed, the Kruskal-Wallis test (for comparison > 2 datasets) or Mann-Whitney U test (for 2 datasets, $p<0.05$ two tailed) were used to identify whether there was difference in parameter concentrations between each operational condition. The correlation between each water quality parameter and operational conditions was determined by calculating the non-parametric Spearman's rank correlation coefficients.

2. Results

2.1 On-going nitrification responses to changing hydraulics

2.1.1 Water quality

As shown in **Table 2**, the pH varied little for all the flow cells running at different hydraulic regimes. Together with the increase in TOC concentration and HPC number in all flow cell units, the turbidity in every flow cell at each flow rates increased at the end of the tests. As the nitrification process had been established before the tests, the concentration of total nitrogen dropped after the tests in all experimental conditions.

The effect of hydraulic regimes on these five water quality parameters was identified based on the Mann-Whitney U test (**Table S1 and S2**). Along with the experiments, there were statistical differences in pH values and TOC concentrations between each hydraulic regime when the total Cl_2 was 5 mg/L. For flow cells fed with water of 1 mg/L total Cl_2 in test phase 2, pH in the flow cell operated at 10 L/min was observed to be different between that in flow cells running at other two flow rates. Changing hydraulic regimes resulted in significant difference in TN levels under several conditions, while there was no statistical difference in HPC observed between any experimental scenario. When the Cl_2/NH_3-N mass ratio was 5:1 in test phase 2, the water was observed to be more turbid in the cell at flow rate of 6 L/min than that in the units at the other two hydraulic regimes under both disinfectant concentrations (**Table 2**). Further explanations for this observation are given in the discussion section (Sec. 3.3).

Analysis of *Fm* was made for each flow cell unit. From the results shown in **Table 3**, the majority of the *Fm* values are < 1 and the change pattern during the experiment is different for each scenario. In most cases, the largest value of *Fm* occurred during the

middle stage of the tests (around days 16 ~ 21). However, no significant difference was found in the ratios between different hydraulic regimes (**Table S1 and S2**).

2.1.2 Indicators of nitrification

Figure 2 and Figure 3 show the change in concentrations of free Cl_2, NH_3-N, NO_3^--N and NO_2^--N within flow cell units under different scenarios for each test phase. For total Cl_2 and monochloramine, the monitoring results are provided in **Table S4** and **S5** and the detection limit of total/free chlorine in this study is 0.02 mg/L. As shown in Fig.2 and 3, the disinfectant residual (free Cl_2) under most of the operational conditions decreased sharply at the early stage of the experiment and the residual was at low level (<0.1 mg/L) till the end of tests.

No significant difference in free Cl_2 was found between different hydraulic regimes, except when the total chlorine and Cl_2/NH_3-N ratio were 5 mg/L and 5:1 in the feed water. Under this condition, the concentration of free Cl_2 in cell running at 10 L/min was significantly higher than that at 6 L/min (**Table S1 and S2**).

Although nitrification within each flow cell unit was established under the same incubating condition, the change in nitrification episodes (NH_3-N, NO_3^--N and NO_2^--N) was not constant under different flow rates during the test phases. Overall, the concentrations of nitrite increased under different hydraulic conditions, but the pattern of changes were different (**Fig. 2a, b and Fig. 3a, b**). In contrast, the concentration of nitrate-nitrogen within flow cell operated at all flow rates showed a declining trend. It should be noted that although the concentration of nitrite-nitrogen in flow cell operating at the flow rate of 10 L/min (**Fig. 3c, f**) was maintained at a relative low level during the first 20 days of the test phase 2, the concentration increased sharply at the later stage of experiment.

Compared with phase 1, hydraulic regimes showed more impact on nitrification related parameters in test phase 2. As the concentration of NO_2^--N is commonly applied as an indicator of nitrification, a boxplot was made to present the data of NO_2^--N for each experiment scenario (**Fig. 4**) and to evaluate hydraulic condition effects on the nitrification process. Based also on the results from Mann-Whitney U test (**Table S1 and S2**), the concentration of NO_2^--N was found to be statistically higher in flow cells running at the flow rate of 6 L/min in test phase 2 (**Fig. 4**). In comparison, the hydraulic regimes did not show similar impacts on the production of nitrite in test phase 1.

2.2 Response to different disinfection strategies

2.2.1 Water quality response

Where the Cl_2/NH_3-N ratio was 5:1, more significant water quality differences were found between the different hydraulic regimes (**Table 2**). The concentration of disinfectant dose in feed water affected the pH and TOC in flow cells operated at the flow rate of 2 and 6 L/min (**Table S1 and S3**). Under these two hydraulic regimes, pH was lower in flow cell fed with higher concentration of disinfectant, while the TOC was higher when an increasing disinfectant dose was applied. Different disinfection scenarios did not show effect on HPC (**Table 2**) and the microbiological decay factor (**Table 3**).

2.2.2 On-going nitrification evaluation

At the end of the two test phases, disinfectant residual declined to a quite low level (<0.1 mg/L) under all disinfection scenarios. In contrast to rapid declines in free chlorine within all flow cells at the beginning of the experiment in test phase 1, the concentration of free chlorine in flow cells running at 2 L/min and 10 L/min could be maintained at a reasonable level (around 1 mg/L) during the first 20 days in test phase 2 (**Fig. 3d, f**). Throughout the same period in test phase 2, less nitrite accumulated and ammonia loss were observed in flow cells operated at 2 L/min and 10 L/min as well. Compared with different disinfectant dose concentrations, greater reduction in nitrate (average loss of 85%) was observed when the total chlorine was 5 mg/L in feed water (**Fig. 2 and 3**).

As shown in **Fig. 4**, the disinfectant dose did affect the production of nitrite under several hydraulic conditions (i.e. 6 L/min and 10 L/min). However, this impact did not show a constant effect under different Cl_2/NH_3-N levels. When the ratio was 3:1, nitrite accumulation was promoted in flow the cell fed with a lower concentration of disinfectant. An opposite trend was observed in test phase 2, where the ratio was 5:1 in feed water (**Fig. 4**).

2.3 Assessment of biofilm EPS structure

Figure 5 shows the extracellular carbohydrate and protein concentrations of the isolated biofilm. To compare their properties, concentration is expressed as μg per total organic carbon (mg) detected within the samples. Within the isolated biofilm, carbohydrate was the dominant component and varied under different operational conditions. The peak value

of extracellular carbohydrate was obtained from biofilm isolated from flow cell with flow rate at 6L/min when the total chlorine in feed water was 1 mg/L. However, when the concentration of monochloramine was 5mg/L in both test phases, the carbohydrate concentration was found to increase with increasing hydraulic regimes.

Table 4 shows the details of total extracellular protein and carbohydrate content produced by cell mass, and the ratio of total EPS mass (calculated by adding protein and carbohydrate together) and cell numbers. The ratio of carbohydrate to protein in sampled biofilm fluctuated with operational conditions (from 2.73 to 16.07). The EPS production ability of isolated biofilm was different between different experimental scenarios. There was a decease (around one order of magnitude) in the EPS-to-cell ratio when the biofilm was isolated from flow cell units operated in test phase 2, where the Cl_2/NH_3-N ratio was 5:1.

2.4 Correlations between water quality parameters

As shown in **Fig. 4**, nitrification was observed in each experimental scenario of this study. In order to identify whether there are correlations between the water quality parameters, and therefore give possible suggestion for monitoring nitrification, a non-parametric correlation analysis was performed. **Figure 6** provides the results of the analysis, which include the Spearman correlation coefficients and the statistical significance for each correlation for the two test phases.

Correlations were identified between most of the selected parameters in the two test phases. As can be seen in **Fig. 6**, NO_2^--N, turbidity and TOC were positively correlated with each other ($p<0.05$). NO_2^--N were observed to be negative correlated with NO_3^--N, NH_3-N and TN ($p<0.01$).

The correlations between NO_2^--N and free Cl_2 were not clear. No statistical correlation was identified in test phase 1, and was found to be negative in test phase 2 ($p<0.01$). In addition, NH_3-N was strongly positively correlated with TN ($p<0.01$), and there were positive correlations between NO_3^--N and NH_3-N and TN within these two test phases.

For microbial parameters, HPC or microbial decay factor (*Fm*) was not correlated with any water quality parameters measured within this study.

3. Discussion

3.1 Hydraulic impacts upon nitrification

In this study, three hydraulic regimes were investigated for their impacts on nitrification within chloraminated flow cell units, which had been incubated with biofilm and had nitrification established before tests were conducted. Although the same incubation conditions were controlled in different flow cell units before testing, significant differences in water quality parameters were found between the cells running at different hydraulic regimes during the test phases (**Table 2**). Since biofilm had been established before testing and the flow rate was the only controlling factor within the single test phase, the hydraulics could be one of the key factors that contributed to the difference in water quality. In addition, since nitrification had been established before testing and significant difference in nitrite concentration was observed after having flow cells operating at different hydraulic conditions during the test phases, the difference in water quality could also be a result of the hydraulic impacts on the nitrification process.

Hydraulic condition is considered to be an influencing factor due to its impact on mass transfer to biofilm, including nutrients, disinfectants, oxygen and microorganisms (Beer et al., 1996; Beyenal and Lewandowski, 2002; Vieira et al., 1993), and also on biofilm density, composition and structural characteristics (Abe et al., 2012; Purevdorj et al., 2002). Both increased mass penetration to biofilm and greater bacterial density were observed within *Pseudomoas fluorescens* culture when incubated with increasing flow velocity (Vieira et al., 1993). Similarly, Lehtola et al. (2006) observed that within pilot distribution system biofilm formation was favoured by increased flow velocity and accompanied with increasing consumption of nutrients.

In the current study, nitrification was observed and as nitrification is a microbial process, the density and activity of both the nitrifiers and heterotrophic bacteria within the biofilm was considered to affect this process. If the theory described above was true, nitrification would be promoted under higher flow rates due to the potential increases in density of nitrifying bacteria in the biofilm. However, as the most common indicator of nitrification, the accumulation of nitrite was observed to be promoted in flow cells running at 6 L/min (**Fig. 4**). In other words, nitrification was suggested to be more severe when the flow rate was 6 L/min, than that in flow cells operating with other two flow rates. In addition, nitrification was found to be inhibited to some degree at the beginning of the test in units running at the flow rate of 10 L/min (**Fig. 2 and 3**). This might be explained by the

315 fact that the increasing flow rate not only promotes the nutrient diffusion (especially
316 ammonia for nitrification) into the biofilm, but it also increases the detachment of biofilm
317 to bulk water and hence reduces the available nitrifiers that participated in the nitrification
318 process. The impact of increasing flow velocity on biofilm removal from surface has been
319 observed by Lehtola et al. (2006) and Sekar et al. (2012), who both found a positive
320 correlation between flow velocity and planktonic cell counts in bulk water. To overcome
321 the detachment force, biofilm tends to respond with an increasing cohesive strength (Paul
322 et al., 2012) and higher microbial growth rates (Dreszer et al., 2013; Liu and Tay, 2001).
323 However, researches also observed that the bacterial growth rate in biofilm tended to
324 increase within a certain flow range but began to decrease when the excessive shear forces
325 would destroy the biofilm structure (Tsai, 2005; Wang et al., 2013). This is supported by
326 current observation that the most possible favourable hydraulic condition for nitrification
327 was the flow rate of 6 L/min. At this hydraulic condition (6 L/min , Re = 3321), the flow
328 turbulence was under the transition stage from laminar to turbulent and the biofilm/nitrifier
329 growth could take full advantage of the increasing mass transfer by flow, while their
330 detachment rate was lower than the growth rate.
331 It has been suggested that biofilm EPS structure and composition are highly affected by
332 the environment in which the biofilm is incubated, and the bacterial communities presented
333 (Ahimou et al., 2007; Simoes et al., 2007). In order to investigate whether the difference
334 in nitrification potential between different hydraulic conditions was caused by hydraulics
335 impact on biofilm structure, the characteristics of biofilm EPS were evaluated within the
336 current study. Carbohydrate was found to be the dominant component of all biofilms from
337 flow cell units (**Fig. 5**), as has also been reported in other studies (Kilb et al., 2003). The
338 carbohydrate/protein mass ratios of biofilm's EPS were all above 1 (**Table 4**) and the value
339 varied with different operational conditions. In most cases, without considering the
340 disinfectant concentration and Cl_2/NH_3-N mass ratio, a higher proportion of carbohydrate
341 was observed in biofilm incubated at flow rate of 6 L/min, suggesting that carbohydrate
342 synthesis was promoted (**Table 4**). In combination with the observation that nitrite
343 production was promoted when flow rate was 6 L/min, it is suggested that biofilm EPS
344 composed of more carbohydrate would be conductive to nitrification. EPS carbohydrate
345 concentration was reported to be positively correlated with the biofilm cohesive energy (R^2

= 0.9) (Ahimou et al., 2007). A stable biofilm structure would bring benefit to the aggregated bacteria to overcome outer interference and hence to promote biological related activity.

3.2 Disinfection strategies effects

Monochloramine was produced by the combination of free chlorine and ammonia at a mass ratio of 3:1 or 5:1. A 5 to 1 mass ratio would achieve the maximum formation of monochloramine without free ammonia left, while the 3 to 1 mass ratio would ensure monochloramine to be the dominant form, but will result in an excess of free ammonia in the feed water (Fleming et al., 2005, 2008). Due to the nitrifying biofilm been established during the incubation stage within the current study, the higher Cl_2/NH_3 mass ratio was supposed to control nitrification due to the limited amount of free ammonia available (Fleming et al., 2005, 2008). In terms of inhibiting nitrification, neither of these two ratios could control the process continually, and this is in agreement with an industry survey made by Wilczak et al. (1996). However, when considering nitrite data in conjunction with the free ammonia nitrogen data (**Fig. 2 and 3**), it was noted that at the beginning of test phase 1 ammonia level dropped after a corresponding increase in nitrite concentration, but a converse observation was found in test phase 2. The difference is suggested to be caused by whether free ammonia is the major form of total ammonia within water. When the Cl_2/NH_3-N mass ratio was 3:1, the extra free ammonia in bulk water would firstly be consumed if nitrification process was on-going, and hence a decrease of free ammonia concentration would be observed. In contrast, due to no free ammonia existing when the Cl_2/NH_3-N mass ratio was 5:1, free ammonia would be released from monochloramine either by auto-decomposition or reactions between organic or inorganic species (Valentine 1998). Once nitrification occurred, the release of free ammonia would be promoted, and its concentration would increase if the consumption rate was less than the production. Although the initial increase of ammonia before nitrification was reported in previous studies (Liu et al., 2005; Yang et al., 2008), no explicit discussion on this has been provided. From the results of current study, the Cl_2/NH_3-N mass ratio is a factor that should be considered, especially for utilities using ammonia as nitrification indicator.

When the total Cl_2 maintained in feed water was 1 mg/L within these two test phases, the free Cl_2 dropped significantly (close to 0.1 mg/L) at the beginning of tests and remained

consistently low (<0.05 mg/L) in all conditions. Considering nitrifying biofilm had been established before the tests, the rapid loss of disinfectant is suggested to be the result of reactions involving nitrifiers and heterotrophic bacteria. In addition, the uninhibited nitrification would further increase the decay rate of chloramine (Cunliffe, 1991) and hence result in a continuous low level of chloramine. The concentration of total chlorine in feed water was changed to 5 mg/L for investigating whether nitrification could be controlled by higher disinfectant dose. Liu et al. (2005) suggested that nitrification rarely occurred when disinfectant residual was above 1 mg/L and Cl_2/NH_3-N mass ratio was greater than 5. However, in the current study though nitrification has been inhibited for a period within some instances, especially when the Cl_2/NH_3-N mass ratio was 5 (**Fig. 3d and f**), an increase of nitrite was monitored after the drop of chloramine residuals. Once nitrification occurred, the produced nitrite further accelerated the decay of chloramine and the disinfectant residual decreased to a low level. This could be explained by the high resistance ability of nitrifiers to disinfectant, which was observed to survive in the system with more than 5 mg/L monochloramine dose (Cunliffe, 1991). Furthermore, in flow cells running at the flow rate 6 L/min, the chlorine residual declined extremely fast at the beginning of the test and the nitrification process could not be controlled at all (**Fig. 3b**). This observation suggested that hydraulic regime could be another factor inhibiting the disinfection efficiency, as the nitrite production rate is high enough to consume chloramine and hence accelerate disinfectant decay under a specific range of hydraulic conditions (Eq.(4) and (5)). The results in the current study showed that increasing chloramine amount is an inefficient control method, and this has also been reported in full-scaled utilities experiencing nitrification, where disinfectant residuals could not be regained easily once lost and the activity of nitrifying bacteria was observed to increase simultaneously (Odell et al., 1996). The difficulty in controlling on-going nitrification was emphasized in the current study and a long-term efficient management method is urgently required.

$$NH_3 + O_2 \longrightarrow NO_2^- + 3H^+ + 2e^- \quad (4)$$

$$NH_2Cl + NO_2^- + H_2O \longrightarrow NH_3 + NO_3^- + HCl \quad (5)$$

On the other hand, the disinfectant strategy might influence biofilm biomass and EPS per cell in terms of bacterial activity and EPS availability. A higher concentration of disinfectant was hypothesized to have better disinfectant efficiency for controlling biomass

within biofilm. However, from **Table 4**, in test phase 2, the biomass in biofilm conditioned by higher concentration of chloramine (5 mg/L) was greater than that in biofilm from flow cells fed with lower disinfectant (1 mg/L), while a reverse relationship was observed for EPS per cell. One of the functions of EPS is to protect biofilm against environmental stress (Weiner et al., 1995). Xue et al. (2013) suggested two mechanisms of EPS protection role on bacteria inactivity by both chlorine and chloramine. The authors suggested EPS might work as either disinfectant consumer (for chlorine inactivation) or limiter that prevents the access of chloramine to the cell membrane (Xue et al., 2013). In the current study, since nitrification was observed and this process would accelerate the decomposition of chloramine to free chlorine and ammonia (Oldenburg et al., 2002), hence the disinfectant affecting biofilm might be the combination of chloramine and chlorine. If the mechanisms described above are true, then the increased EPS produced would consume the free chlorine and also work as protector to increase biofilm resistance ability to chloramine. Once the available disinfectant residual was consumed by EPS, nitrifiers within biofilm could utilize free ammonia to create nitrite. This partly explains why the concentration of nitrite increased when free chlorine dropped to a low level (**Fig. 3c and f**).

3.3 Water quality parameters related to nitrification

To verify the observation discussed above, other water quality parameters related to nitrification potential were evaluated. Previous studies suggested parameters including pH, turbidity, disinfectant residual, NH_3-N, NO_3^--N, TOC and HPC were related to nitrification process (Liu et al., 2005; Odell et al., 1996; Wilczak et al., 1996; Wolfe and Lieu, 2003; Yang et al., 2008). Within this study, parameters including TOC, turbidity, NH_3-N, NO_3^--N and TN were observed to have correlation with nitrite production (**Fig. 6**). The organic carbon within drinking water system was suggested to be an indirect stimulating factor in terms of nitrifying bacteria growth, as it could react with chloramine and further reduce the inactivation of nitrifier and support the formation of biofilm (Kirmeyer et al., 1995; Zhang et al., 2010). Based on the water quality data from feed water for the current experiment (**Table S3**), the TOC within source water was around 1~2 mg/L. During the tests, there was an increase of organic carbon in bulk water under all operational conditions (**Table 2**). The source of increasing organic carbon in drinking water system was thought to be the result of increasing HPC in water (**Table 2**), and also the release of microbial metabolism

materials (Noguera et al., 2009; Wolfe et al., 1990; Yang et al., 2008). Similar to the correlation analysis results within the current study, positive correlation between nitrifying bacteria and TOC level was observed as suggested by Zhang et al. (2010), who fed a simulated drinking water system with high/low TOC chloraminated water and the results indicated that nitrification was promoted under higher concentration of TOC. Therefore, the level of TOC in bulk water might be used as an indicator of nitrification potential.

Turbidity is a water quality indicator, which is caused by the presence of suspended materials, such as clay, silt, organic or inorganic matter, plankton and other microscopic organisms (McCoy and Olson, 1986). This was verified from the observation that a significant positive correlation existed between TOC and turbidity in the current study (**Fig. 6**). In addition, turbidity was suggested to be an indicator of nitrification as well. Lipponen et al. (2002) reported an increase of turbidity associated with increasing number of nitrifying bacteria in an investigation within 15 chloraminated DWDSs. Although the nitrifying bacteria was not measured within the current study, strong positive correlation between nitrite and turbidity was found (**Fig. 6**). Together with the observation of the change pattern of nitrite, TOC and turbidity in flow cell units running at different flow rates, these two parameters followed similar trend between different hydraulic conditions (**Fig. S1 and S2**). This was different from previous study, which observed increasing turbidity was associated with the detachment of materials from pipe surface caused by increased flow velocity (or shear stress) (Husband et al., 2008). This difference might provide further evidence that the water quality within the current study was mostly affected by hydraulic impacts on nitrification process, rather than directly by the hydraulics itself.

Microbial decay factor (*Fm* ratio) was firstly introduced by Sathasivan et al. (2005), who suggested this factor could indicate the presence of AOB activity by determining microbial contribution to total chloramine decay (Sathasivan et al., 2008). Based on this, an increase of *Fm* ratio would be observed to be associated with the occurrence of nitrification, and its value could reflect the nitrification potential to some extent. Within the current study, similar to the results from a batch test made by Sawade et al. (2016), the increases of *Fm* ratio was monitored in some cases where nitrite concentration increased (**Table 3**), however, no significant correlation was found between its value and nitrite (**Fig. 6**). In addition, low value of *Fm* (< 0.1) was observed in cell units with severe nitrification,

suggesting that this factor might not be an effective tool to predict nitrification. Considering the mechanism of this method, which assumed AOB activity was the main microbiological cause of chloramine decay, the results obtained in the current study do not seem to be in agreement with the suggested mechanism. The low value of *Fm* ratio in conditions with severe nitrification (nitrite > 0.05 mg/L) might have resulted from high concentration of soluble microbial products remaining within the water sample (Krishna et al., 2012), and oxidation reactions between chloramine and nitrite (Krishna and Sathasivan, 2010).

3.4 Suggestions for controlling nitrification

Combined with the discussion above, the hydraulics was supposed to have an impact on nitrification, but the influence could not be explained by simple linear relationship. Nitrification will be more severe when the potential for promoting it from hydraulic to nitrifying bacteria growth within biofilm was greater than the detachment force brought by increasing shear force. To better understand the phenomenon, the abundance of nitrifying bacteria is suggested to be monitored along the test in further research. Based on the results from this study, the utilities are suggested to pay more attention to maintaining the disinfectant residuals within the systems when the flow turbulence (*Re* number) is around 3300, in which case the nitrification is to be more likely to occur and become severe.

Although nitrification was observed under all operational conditions within the current study, increasing the flow rate to turbulent conditions and increasing the disinfectant dose concentration with high Cl_2/NH_3-N mass ratio (5:1) simultaneously within chloraminated DWDSs could still be considered as a joint method for controlling nitrification. Lower flow rate was not proposed (i.e. 2 L/min) for the reason that other water quality problems could be associated with increase of hydraulic retention time (Machell et al., 2009; Tinker et al., 2009), although the level of nitrite produced under the lower flow rate was relatively low based on the current results. The failure to inhibit nitrification for a long-term in flow cells operated with flow rate of 10 L/min and fed with 5 mg/L monochloramine within the current study was thought to be due to the long water age (3 days), which would increase the auto-decomposition of disinfectant. This water age was chosen for the purpose of magnifying the physico-chemical changes of water quality under different operational conditions. To further verify the proposed management method, shorter water age is required to minimize the decline in disinfectant residual caused by the extended residence

time (Machell et al., 2009). In addition, as turbulent flow (flow rate = 10 L/min, *Re* = 5535) was suggested to inhibit nitrification process to some degree within the current experimental facility, this fluid condition could be considered for reducing biologically mediated monochloramine during the maintenance phase in real systems.

4. Conclusion

This study provided new information on the effect from hydraulic regimes and disinfection strategies on nitrification process within chloraminated DWDS. The findings highlight the difficulty in controlling nitrification, but also provide information for water utilities to propose possible nitrification control methods. The outcomes of this study are summarized below:

- Hydraulic effects on the nitrification process and nitrite accumulation were observed and these processes were promoted when the flow rate was 6 L/min, and where the fluid transforms from the laminar to the turbulent flows.
- Increasing Cl_2/NH_3-N mass ratio was not considered as an effective nitrification control strategy. The different responses of ammonia to the change of nitrite observed between these two ratios (3:1 and 5:1) might explain why the changing pattern of ammonia varied in different utilities before nitrification.
- Increasing total chlorine concentration was found to inhibit nitrification for a short period in some cases, while it was completely inefficient in the cell running at the flow rate of 6 L/min. Combined with the less severe nitrification that was observed in the flow cells operated at higher flow rate (10L/min), a joint action is suggested to control nitrification by increasing both flow turbulence and chloramine concentration within DWDS with short water age.
- Water quality parameters including TOC, turbidity, NH_3-N, nitrate and TN were found to be related to nitrification process. Specifically, except monitoring the change of nitrite, the variation of TOC and turbidity is suggested to be potential effective to evaluate nitrification extent also.
- Carbohydrate was the dominant composition of the biofilm EPS in this study and the carbohydrate/protein ratio was found to be higher in biofilm extracted from flow cell units experiencing more severe nitrification. This suggests biofilm with stronger cohesive ability would be conductive to nitrification.

532 • More biomass, but less EPS per cell was observed in biofilm conditioned under
533 higher concentration of disinfectant dose (5 mg/L), suggesting the disinfection resistant
534 ability of EPS to outer interference would be one of the factors that result in the difficulty
535 to inhibit nitrification within DWDS.

Conflicts of interest

There are no conflicts to declare.

Acknowledgements

The authors would like to acknowledge the technical support from the technicians at the School of Engineering, Cardiff University. We would also want to thank Dr. Gordon Webster for assisting on EPS analysis.

Appendix A: Supplementary data

Supplementary data associated with this article can be found in the online version at XXXX.

Reference

Abe, Y, Skali-Lami, S, Block, J-C, Francius, G, 2012. Cohesiveness and hydrodynamic properties of young drinking water biofilms. Water Research 46:1155-1166.

Ahimou, F, Semmens, M J, Haugstad, G, Novak, P J, 2007. Effect of protein, polysaccharide, and oxygen concentration profiles on biofilm cohesiveness. Appl. Environ. Microbiol. 73:2905-2910.

APHA, 1998. Standard Methods for the Examination of Water and Wastewater. 20th ed Am. Public Health Assoc, Washington, DC.

Beer, D D, Stoodley, P, Lewandowski, Z, 1996. Liquid flow and mass transport in heterogeneous biofilms. Water research 30:2761-2765.

Beyenal, H, Lewandowski, Z, 2002. Internal and external mass transfer in biofilms grown at various flow velocities. Biotechnology progress 18:55-61.

Brown, M J, Lester, J N, 1980. Comparison of bacterial extracellular polymer extraction methods. Appl. Environ. Microbiol 40:179-185.

Cunliffe, D A, 1991. Bacterial nitrification in chloraminated water supplies. Appl. Environ. Microbiol 57:3399-3402.

Douterelo, I, Sharpe, R, Boxall, J, 2013. Influence of hydraulic regimes on bacterial community structure and composition in an experimental drinking water distribution system. Water Research 47:503-516.

Dreszer, C, Vrouwenvelder, J S, Paulitsch-Fuchs, A H, Zwijnenburg, A, Kruithof, J C, Flemming, H C, 2013. Hydraulic resistance of biofilms. Journal of Membrane Science 429:436-447.

Fish, K, Osborn, A, Boxall, J, 2016. Characterising and Understanding the Impact of Microbial Biofilms and the Extracellular Polymeric Substance (EPS) Matrix in Drinking Water Distribution Systems.

Fish, K, Osborn, A, Boxall, J, 2017. Biofilm structures (EPS and bacterial communities) in drinking water distribution systems are conditioned by hydraulics and influence discolouration. Science of the Total Environment 593:571-580.

Fleming, K K, Harrington, G W, Noguera, D R, 2005. Nitrification potential curves: a new strategy for nitrification prevention. American Water Works Association 97:90-99.

Fleming, K K, Harrington, G W, Noguera, D R, 2008. Using nitrification potential curves to evaluate full-scale drinking water distribution systems. American Water Works Association 100:92.

Furumai, H, Rittmann, B, 1994. Evaluation of multiple-species biofilm and floc processes using a simplified aggregate model. Water Science Technology 29:439.

Gagnon, G, O'Leary, K, Volk, C, Chauret, C, Stover, L, Andrews, R, 2004. Comparative analysis of chlorine dioxide, free chlorine and chloramines on bacterial water quality in model distribution systems. Journal of environmental engineering 130:1269-1279.

Hoefel, D, Monis, P T, Grooby, W L, Andrews, S, Saint, C P, 2005. Culture-independent techniques for rapid detection of bacteria associated with loss of chloramine residual in a drinking water system. Appl. Environ. Microbiol 71:6479-6488.

Husband, P, Boxall, J, Saul, A, 2008. Laboratory studies investigating the processes leading to discolouration in water distribution networks. Water Research 42:4309-4318.

Kilb, B, Lange, B, Schaule, G, Flemming, H-C, Wingender, J, 2003. Contamination of drinking water by coliforms from biofilms grown on rubber-coated valves. International Journal of Hygiene environmental Health 206:563-573.

Kirmeyer, G J, Odell, L H, Jacangelo, J, Wilczak, A, Wolfe, R, 1995. Nitrification occurrence and control in chloraminated water systems. AWWA Res. Fdn., Denver.

Krishna, K B, Sathasivan, A, 2010. Does an unknown mechanism accelerate chemical chloramine decay in nitrifying waters? Journal-American Water Works Association 102:82-90.

Krishna, K B, Sathasivan, A, Sarker, D C, 2012. Evidence of soluble microbial products accelerating chloramine decay in nitrifying bulk water samples. Water Research 46:3977-3988.

LeChevallier, M W, Lowry, C D, Lee, R G, 1990. Disinfecting biofilms in a model distribution system. American Water Works Association 82:87-99.

Lehtola, M J, Laxander, M, Miettinen, I T, Hirvonen, A, Vartiainen, T, Martikainen, P J, 2006. The effects of changing water flow velocity on the formation of biofilms and water quality in pilot distribution system consisting of copper or polyethylene pipes. Water research 40:2151-2160.

Lieu, N I, Wolfe, R L, III, E G M, 1993. Optimizing chloramine disinfection for the control of nitrification. American Water Works Association 85:84-90.

Lipponen, M T, Suutari, M H, Martikainen, P J, 2002. Occurrence of nitrifying bacteria and nitrification in Finnish drinking water distribution systems. Water Research 36:4319-4329.

Liu, S, Taylor, J S, Randall, A, Dietz, J D, 2005. Nitrification modeling in chloraminated distribution systems. American Water Works Association 97:98-108.

Liu, Y, Tay, J H, 2001. Metabolic response of biofilm to shear stress in fixed-film culture. Journal of Applied Microbiology 90:337-342.

Machell, J, Boxall, J, Saul, A, Bramley, D, 2009. Improved representation of water age in distribution networks to inform water quality. Journal of Water Resources Planning Management 135:382-391.

McCoy, W F, Olson, B H, 1986. Relationship among turbidity, particle counts and bacteriological quality within water distribution lines. Water Research 20:1023-1029.

Mi, Z, Dai, Y, Xie, S, Chen, C, Zhang, X, 2015. Impact of disinfection on drinking water biofilm bacterial community. Journal of Environmental Sciences 37:200-205.

Noguera, D, Goel, R, Harrington, G, Yilmaz, L, 2009. Identification of Heterotrophic Bacteria that Colonize Chloraminated Crinking Water Distribution Systems. Water Environment Research Foundation.

Norton, C D, LeChevallier, M W, 1997. Chloramination: its effect on distribution system water quality. American Water Works Association 89:66-77.

Odell, L H, Kirmeyer, G J, Wilczak, A, Jacangelo, J G, Marcinko, J P, Wolfe, R L, 1996. Controlling nitrification in chloraminated systems. American Water Works Association 88:86-98.

Oldenburg, P S, Regan, J M, Harrington, G W, Noguera, D R, 2002. Kinetics of Nitrosomonas europaea inactivation by chloramine. American Water Works Association 94:100-110.

Paul, E, Ochoa, J C, Pechaud, Y, Liu, Y, Liné, A, 2012. Effect of shear stress and growth conditions on detachment and physical properties of biofilms. Water Research 46:5499-5508.

Pintar, K D, Slawson, R M, 2003. Effect of temperature and disinfection strategies on ammonia-oxidizing bacteria in a bench-scale drinking water distribution system. Water Res 37:1805-1817.

Purevdorj, B, Costerton, J W, Stoodley, P, 2002. Influence of hydrodynamics and cell signaling on the structure and behavior of Pseudomonas aeruginosa biofilms. Appl. Environ. Microbiol. 68:4457-4464.

Sathasivan, A, Fisher, I, Kastl, G, 2005. Simple method for quantifying microbiologically assisted chloramine decay in drinking water. Environ Sci Technol 39:5407-5413.

Sathasivan, A, Fisher, I, Tam, T, 2008. Onset of severe nitrification in mildly nitrifying chloraminated bulk waters and its relation to biostability. Water Res 42:3623-3632.

Sawade, E, Monis, P, Cook, D, Drikas, M, 2016. Is nitrification the only cause of microbiologically induced chloramine decay? Water Res 88:904-911.

Seidel, C J, McGuire, M J, Summers, R S, Via, S, 2005. Have utilities switched to chloramines? American Water Works Association 97:87-97.

Sekar, R, Deines, P, Machell, J, Osborn, A, Biggs, C, Boxall, J, 2012. Bacterial water quality and network hydraulic characteristics: a field study of a small, looped water

distribution system using culture-independent molecular methods. Journal of Applied Microbiology 112:1220-1234.

Shi, Y, Babatunde, A, Bockelmann-Evans, B, Webster, G, 2019. Influence of hydraulic regimes and Cl 2/NH 3-N mass ratios on the bacterial structure and composition in an experimental flow cell chloraminated drinking water system. Environmental Science: Water Research & Technology 5:977-992.

Simoes, M, Pereira, M O, Sillankorva, S, Azeredo, J, Vieira, M J, 2007. The effect of hydrodynamic conditions on the phenotype of Pseudomonas fluorescens biofilms. Biofouling 23:249-258.

Skadsen, J, Cohen, Y K, 2006. Operational and treatment practices to prevent nitrification. Manual of water supply practices M 56.

Tarre, S, Green, M, 2004. High-rate nitrification at low pH in suspended-and attached-biomass reactors. Appl. Environ. Microbiol 70:6481-6487.

Tinker, S C, Moe, C L, Klein, M, Flanders, W D, Uber, J, Amirtharajah, A, Singer, P, Tolbert, P E, 2009. Drinking water residence time in distribution networks and emergency department visits for gastrointestinal illness in Metro Atlanta, Georgia. Journal of Water Health 7:332-343.

Tsai, Y-P, 2005. Impact of flow velocity on the dynamic behaviour of biofilm bacteria. Biofouling 21:267-277.

Vieira, M, Oliveira, R, Melo, L, Pinheiro, M M, Martins, V, 1993. Effect of metallic ions on the adhesion of biofilms formed by Pseudomonas fluorescens. Colloids Surfaces B: Biointerfaces 1:119-124.

Volk, C J, LeChevallier, M W, 1999. Impacts of the reduction of nutrient levels on bacterial water quality in distribution systems. Appl. Environ. Microbiol 65:4957-4966.

Wang, C, Miao, L, Hou, J, Wang, P, Qian, J, Dai, S, 2013. The effect of flow velocity on the distribution and composition of extracellular polymeric substances in biofilms and the detachment mechanism of biofilms. Water Science and Technology 69:825-832.

Weiner, R, Langille, S, Quintero, E, 1995. Structure, function and immunochemistry of bacterial exopolysaccharides. Journal of industrial microbiology 15:339-346.

Wilczak, A, Jacangelo, J G, Marcinko, J P, Odell, L H, Kirmeyer, G J, 1996. Occurrence of nitrification in chloraminated distribution systems. American Water Works Association 88:74-85.

Wolfe, R L, Lieu, N I, 2001. Nitrifying bacteria in drinking water. Encyclopedia of Environmental Microbiology.

Wolfe, R L, Lieu, N I, 2003. Nitrifying bacteria in drinking water. Encyclopedia of Environmental Microbiology.

Wolfe, R L, Lieu, N I, Izaguirre, G, Means, E G, 1990. Ammonia-oxidizing bacteria in a chloraminated distribution system: seasonal occurrence, distribution and disinfection resistance. Appl. Environ. Microbiol. 56:451-462.

Xue, Z, Hessler, C M, Panmanee, W, Hassett, D J, Seo, Y, 2013. Pseudomonas aeruginosa inactivation mechanism is affected by capsular extracellular polymeric substances reactivity with chlorine and monochloramine. FEMS microbiology ecology 83:101-111.

Xue, Z, Sendamangalam, V R, Gruden, C L, Seo, Y, 2012. Multiple roles of extracellular polymeric substances on resistance of biofilm and detached clusters. Environ Sci Technol 46:13212-13219.

Yang, J, Harrington, G W, Noguera, D R, 2008. Nitrification modeling in pilot-scale chloraminated drinking water distribution systems. Journal of Environmental Engineering 134:731-742.

Zhang, Y, Edwards, M, 2009. Accelerated chloramine decay and microbial growth by nitrification in premise plumbing. American Water Works Association 101:51-62.

Zhang, Y, Griffin, A, Edwards, M, 2008. Nitrification in premise plumbing: role of phosphate, pH and pipe corrosion. Environmental science & technology 42:4280-4284.

Zhang, Y, Griffin, A, Rahman, M, Camper, A, Baribeau, H, Edwards, M, 2009a. Lead contamination of potable water due to nitrification. Environmental science & technology 43:1890-1895.

Zhang, Y, Love, N, Edwards, M, 2009b. Nitrification in drinking water systems. Critical Reviews in Environmental Science and Technology 39:153-208.

Zhang, Y, Zhou, L, Zeng, G, Deng, H, Li, G, 2010. Impact of total organic carbon and chlorine to ammonia ratio on nitrification in a bench-scale drinking water distribution system. Frontiers of Environmental Science Engineering in China 4:430-437.

List of tables

Table 1: Experimental scenarios

Parameters controlled	Cell 1	Cell 2	Cell 3	Cell 4	Cell 5	Cell 6
	Test phase 1					
Water age (days)	3	3	3	3	3	3
Cl_2 dose mg/L	1	1	1	5	5	5
Cl_2:NH_3-N mass ratio	3:1	3:1	3:1	3:1	3:1	3:1
Flow rate (L/min)	2	6	10	2	6	10
Shear stress (N/m^2)	0.018	0.117	0.286	0.018	0.117	0.286
Reynolds number (Re)	1107	3321	5535	1107	3321	5535
Test code	2A_T1	6A_ T1	10A_ T1	2B_ T1	6B_ T1	10B_ T1
	Test phase 2					
Water age (days)	3	3	3	3	3	3
Cl_2 dose mg/L	1	1	1	5	5	5
Cl_2:NH_3-N mass ratio	5:1	5:1	5:1	5:1	5:1	5:1
Flow rate (L/min)	2	6	10	2	6	10
Shear stress (N/m^2)	0.018	0.117	0.286	0.018	0.117	0.286
Reynolds number (Re)	1107	3321	5535	1107	3321	5535
Test code	2A_T2	6A_ T2	10A_ T2	2B_ T2	6B_ T2	10B_ T2

Table 2: Water quality parameters measured before and after tests

Disinfection scenario	Flow rate (L/min)	pH		Turbidity (NTU)		TN (mg/L)		TOC (mg/L)		HPC (logCFU/mL)	
		Day 0	Day 33	Day 0	Day 33	Day 0	Day 33	Day 0	Day 33	Day 0	Day 33
Total Cl_2=1 mg/L	2	7.72	7.73^{a}	0	12	2.91	2.46^{a}	1.68	4.82^{a}	4.08	6.75
Total Cl_2:NH_3-N=3:1	6	7.73	7.65^{b}	2	9^{a}	2.92	2.18^{b}	0.54	2.23	4.22	6.85
	10	7.91	7.52	0	20^{a}	3.00	2.48^{c}	2.61	9.59	4.77	7.41
Total Cl_2=5 mg/L	2	7.60	$7.44^{a,c}$	0	25	5.23	3.36^{a}	0.47	$8.81^{a,b}$	3.95	8.02
Total Cl_2:NH_3-N=3:1	6	7.50	$7.60^{b,d}$	0	6	5.23	4.44^{b}	1.38	4.06	1.56	6.58
	10	7.60	$7.65^{c,d}$	0	7	5.06	4.10^{c}	0.71	3.57^{b}	3.62	6.38
Total Cl_2=1 mg/L	2	7.21	7.74^{e}	5	5^{b}	2.40	$1.54^{d,e}$	0.00	$2.37^{c,d,e}$	4.08	7.06
Total Cl_2:NH_3-N=5:1	6	7.09	$7.73^{f,g}$	0	$15^{b,c}$	2.45	$1.60^{f,g}$	0.00	$5.52^{c,f}$	4.22	7.53
	10	7.21	$7.79^{e,f}$	0	4^{c}	2.63	$1.32^{d,f,h}$	1.89	7.13^{d}	4.77	7.41
Total Cl_2=5 mg/L	2	7.37	$7.65^{h,i}$	2	13^{e}	3.37	1.60^{e}	0.95	$2.81^{e,g,h}$	3.95	7.62
Total Cl_2:NH_3-N=5:1	6	7.14	$7.53^{g,h,j}$	1	$32^{e,f}$	3.52	$2.07^{g,i}$	0.43	$10.28^{f,g,i}$	1.56	7.97
	10	7.31	$7.76^{i,j}$	0	13^{f}	3.47	$0.99^{h,i}$	0.43	$4.14^{h,i}$	3.62	8.02

Value labelled with the same subscript letter indicates that there is significant difference between the data sets collected from different operational conditions throughout the test phases. (Mann-Whitney U test, n=22, $p<0.05$).

Table 3: Monitoring microbial decay factors (*Fm*) for different experimental scenarios during the tests.

Day	2A_T1	6A_T1	10A_T1	2B_T1	6B_T1	10B_T1	2A_T2	6A_T2	10A_T2	2B_T2	6B_T2	10B_T2
1	0.92	0.14	<0.1	0.49	4.91	1.36	N/A	N/A	N/A	N/A	N/A	N/A
6	0.23	14.82	0.14	2.61	1.76	3.15	0.17	1.65	<0.1	3.67	0.10	0.89
9	0.28	0.26	0.25	6.1	0.12	<0.1	1.05	3.80	<0.1	2.30	0.11	0.89
16	2.21	2.16	0.22	0.13	2.61	0.16	<0.1	4.91	<0.1	<0.1	5.33	1.50
21	7.43	7.1	7.87	0.34	<0.1	0.11	1.88	6.12	<0.1	1.05	1.56	0.44
27	4.68	4.51	0.22	0.26	5.79	5.73	1.08	6.38	2.80	0.44	4.28	<0.1
33	<0.1	<0.1	0.32	0.11	2.70	3.72	N/A	N/A	N/A	N/A	N/A	N/A

Table 4: Values of HPC cell numbers, protein, carbohydrate and concentration ratios (EPS) in isolated biofilm from different disinfection scenarios and hydraulic regimes.

Disinfection scenarios	Hydraulic regimes (L/min)	Ratio		Mass		
		EPS:cells (μg/cell)	Carbohydrates:Proteins	Cells	Carbohydrates (μg)	Protein (μg)
Total	2	1.26E-07	2.73	1.80E+07	15.74	5.77
Cl_2=1mg/L	6	1.72E-06	3.64	4.86E+07	65.72	18.05
Cl_2/NH_3-N=3:1	10	1.20E-06	1.17	1.98E+08	13.50	11.50
Total	2	4.70E-06	11.59	3.15E+07	87.06	7.51
Cl_2=5mg/L	6	3.80E-06	14.13	2.34E+07	82.94	5.87
Cl_2/NH_3-N=3:1	10	3.00E-06	5.98	1.98E+07	79.76	13.34
Total	2	4.19E-06	5.21	5.40E+07	27.91	5.36
Cl_2=1mg/L	6	2.18E-07	7.66	2.91E+08	55.99	7.30
Cl_2/NH_3-N=5:1	10	6.16E-07	4.44	6.30E+06	21.55	4.85
Total	2	2.03E-07	16.07	3.55E+08	86.13	5.36
Cl_2=5mg/L	6	1.14E-07	5.35	3.97E+08	38.02	7.10
Cl_2/NH_3-N=5:1	10	2.58E-07	6.78	2.33E+08	41.20	6.08

List of figures

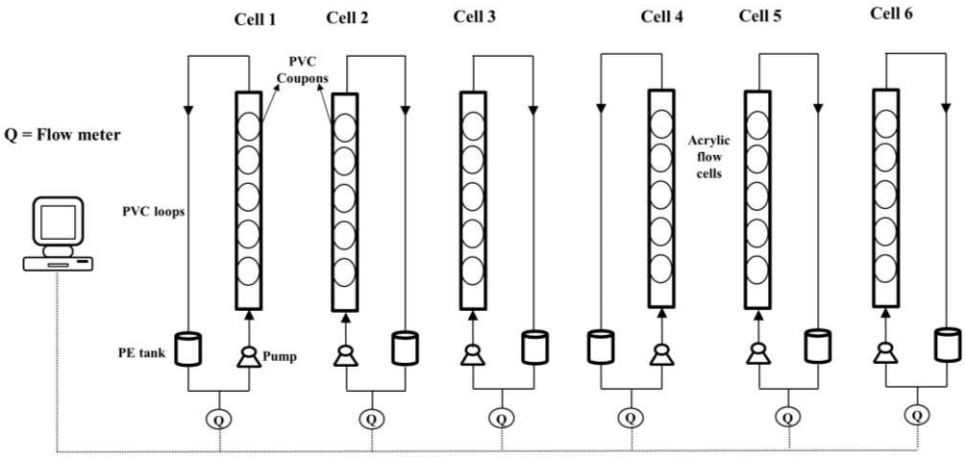

Fig.1: Schematic diagram of the flow cells during test phases

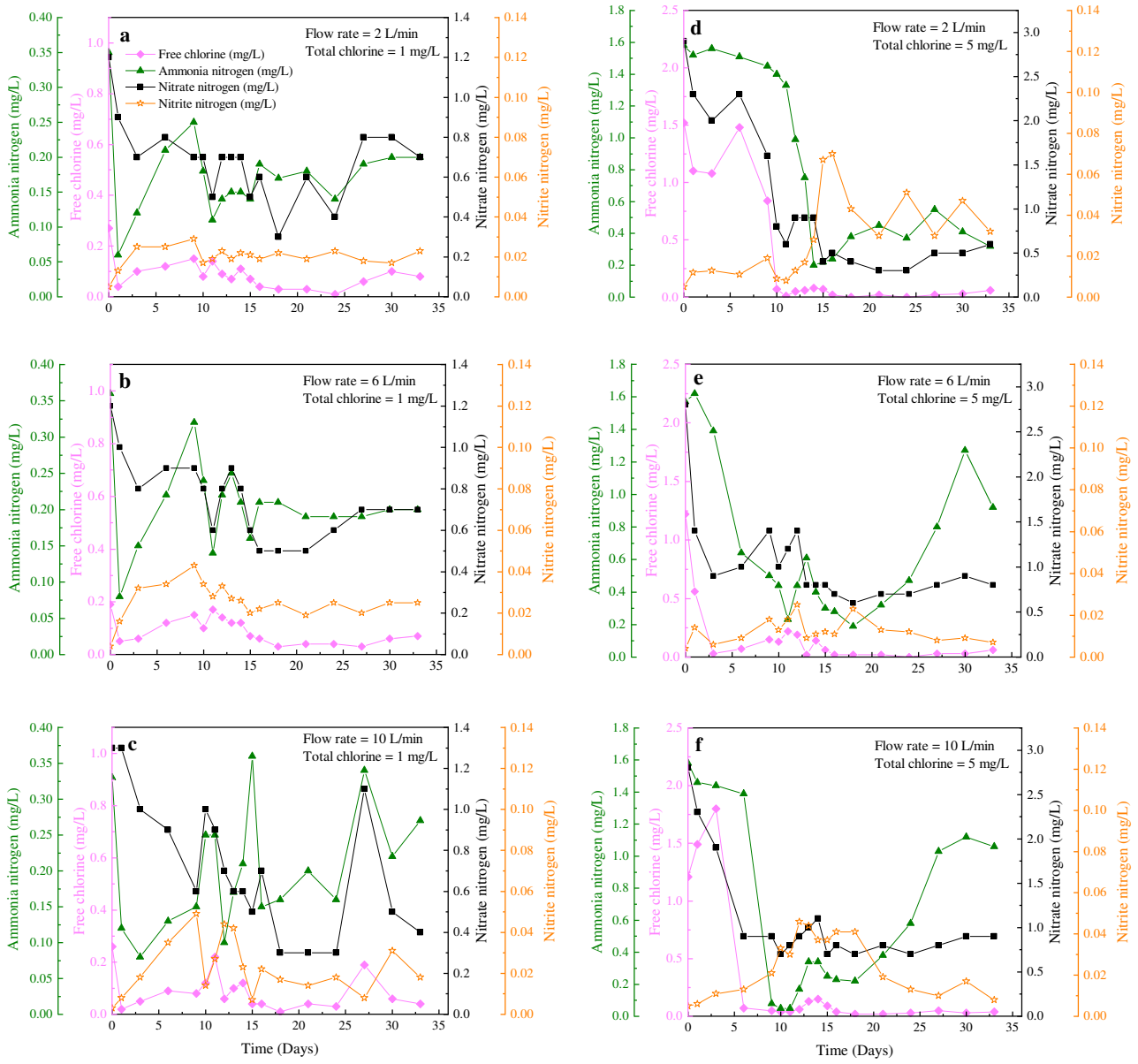

Fig. 1: Time-series plots of free chlorine, nitrite nitrogen, ammonia nitrogen and nitrate nitrogen measured at different hydraulic regimes and disinfection scenarios in test phase 1 (Cl_2/NH_3-N = 3:1). a) flow rate = 2 L/min, total chlorine = 1 mg/L in feed water; b) flow rate = 6 L/min, total chlorine = 1 mg/L in feed water; c) flow rate = 10 L/min, total chlorine = 1 mg/L in feed water; d) flow rate = 2 L/min, total chlorine = 5 mg/L in feed water; e) flow rate = 6 L/min, total chlorine = 5 mg/L in feed water; f) flow rate = 10 L/min, total chlorine = 5 mg/L in feed water.

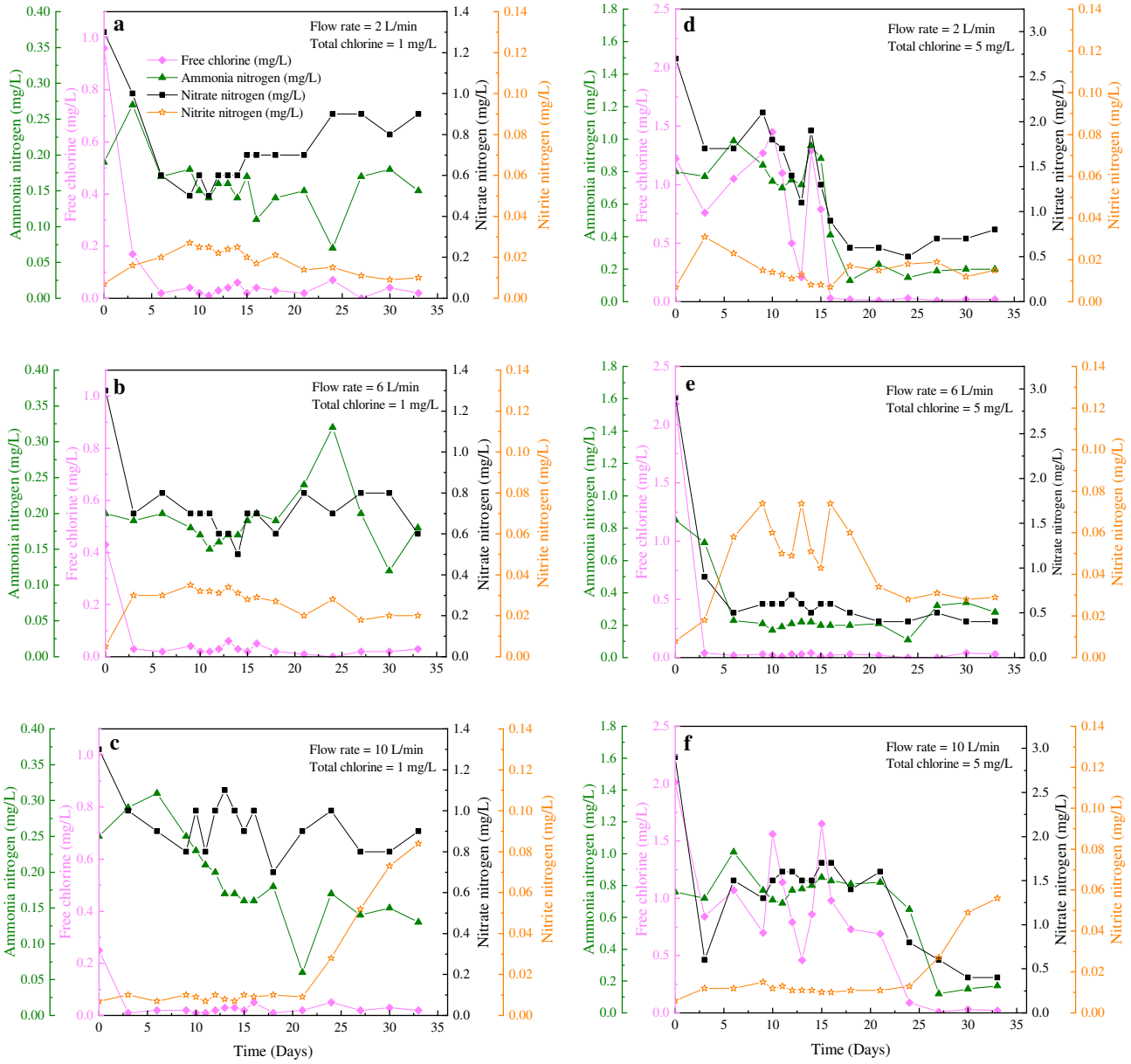

Fig. 2: Time-series plots of free chlorine, nitrite nitrogen, ammonia nitrogen and nitrate nitrogen measured at different hydraulic regimes and disinfection scenarios in test phase 2 (Cl_2/NH_3-N = 5:1). a) flow rate = 2 L/min, total chlorine = 1 mg/L in feed water; b) flow rate = 6 L/min, total chlorine = 1 mg/L in feed water; c) flow rate = 10 L/min, total chlorine = 1 mg/L in feed water; d) flow rate = 2 L/min, total chlorine = 5 mg/L in feed water; e) flow rate = 6 L/min, total chlorine = 5 mg/L in feed water; f) flow rate = 10 L/min, total chlorine = 5 mg/L in feed water.

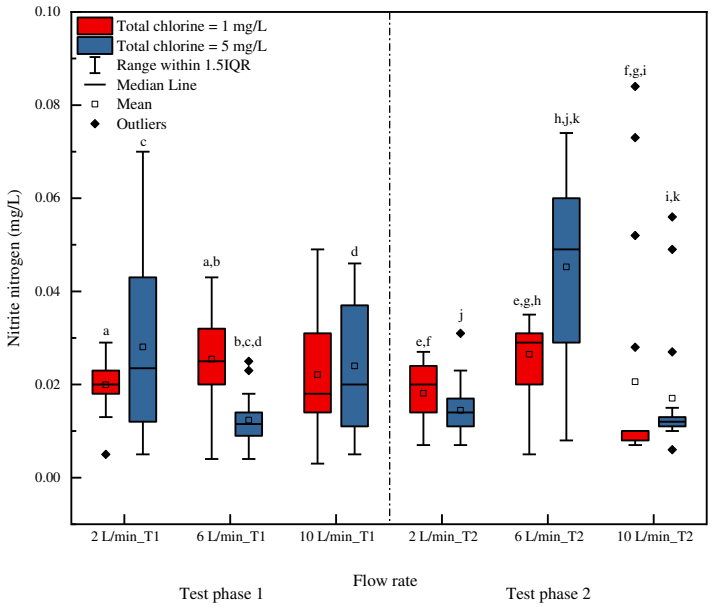

Fig. 4: The concentration of nitrite in different experimental scenarios. The colour represents different total chlorine concentration in feed water. (Value labelled with the same subscript letter indicates that there is significant difference between the data sets collected from different operational conditions. (Mann-Whitney U test, n=22, $p<0.05$)

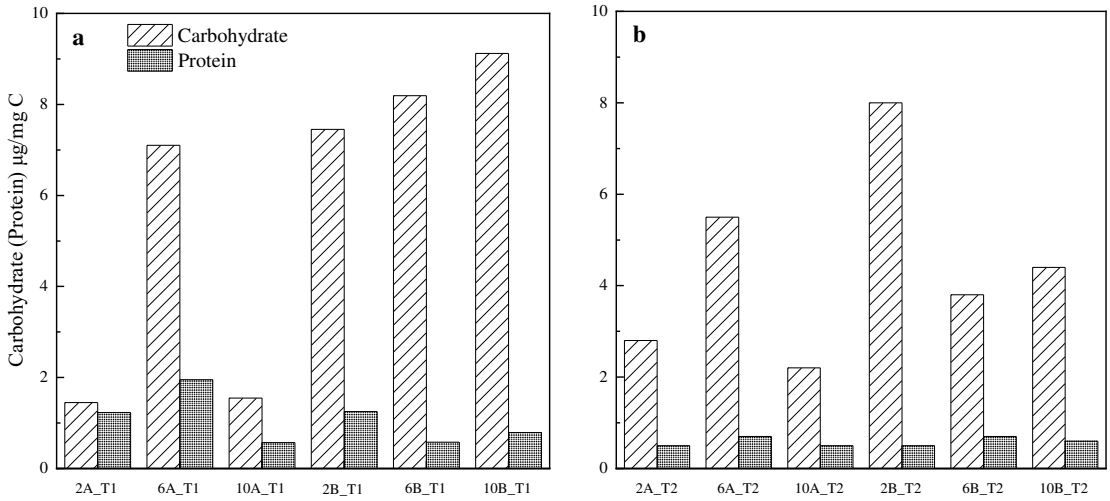

Fig. 5: Total concentration of carbohydrate and protein within EPS of biofilms collected from different flow units. a). EPS extracted from isolated biofilm in test phases 1; b). EPS extracted from isolated biofilm in test phases 2.

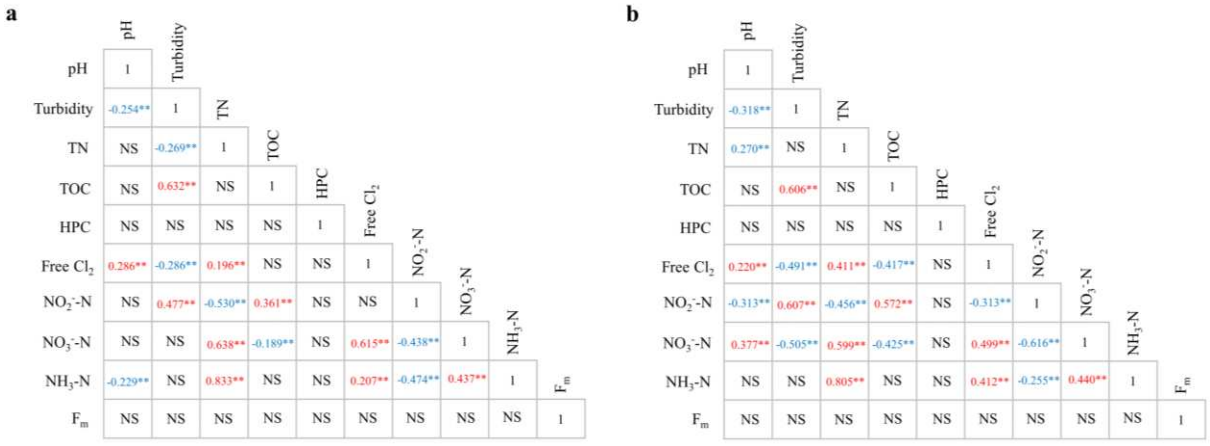

Fig. 6: Non-parametric Spearman correlations between parameters. a) for test phase 1; b) for test phase 2. (n=108 for pH, turbidity, TN, TOC, free Cl_2, NO_2^--N, NO_3^--N, and NH_3-N; n=42 for HPC and n=36 for Fm; **p<0.01, *<0.05; NS = p>0.05; two-tailed test was used.)